Supplement: The UBC ATMOX chamber: An 8 m^3 LED-powered wavelength-dependent modular environmental chamber for indoor and outdoor atmospheric chemistry

Rickey J. M. Lee[1], Ayomide A. Akande[1], Saeid Kamal[2], Paul A. Heine[1], Pritesh Padhiar[3], David Tonkin[4], Wesley Rusinoff[4], Mohamad Rezaei[3,4], and Nadine Borduas-Dedekind[1]

[1]Department of Chemistry, University of British Columbia, Vancouver, V6T 1Z1, Canada
[2]LASIR, Department of Chemistry, University of British Columbia, Vancouver, V6T 1Z1, Canada
[3]Mechanical Engineering Services, Department of Chemistry, University of British Columbia, Vancouver, V6T 1Z1, Canada
[4]Electronic Engineering Services, Department of Chemistry, University of British Columbia, Vancouver, V6T 1Z1, Canada

Correspondence: Nadine Borduas-Dedekind (borduas@chem.ubc.ca)

Contents

S1 Details on the infrastructure and electronics **S3**

S1.1 Chamber pulley system S3

S1.2 Chamber blackout blinds S4

S1.3 Light Characterization S5

S1.4 Pillow bag S6

S1.5 Control Panel S6

S1.6 LED orientation S10

S2 LED Modeling **S10**

S3 Actinometry **S10**

S3.1 Fluorescent experiments S11

S3.2 J_{NO_2} intercomparison S12

S4 Chamber cleaning **S14**

S1 Details on the infrastructure and electronics

S1.1 Chamber pulley system

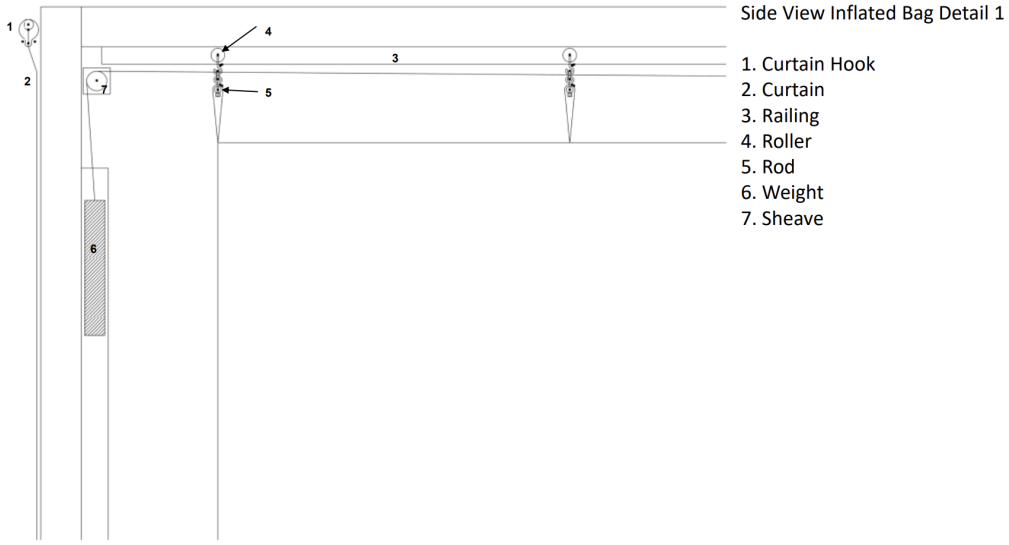

Figure S1. The railing system of the ATMOX chamber is depicted along with its seven components. The bag is held by the rods which are placed onto a roller to move throughout the chamber space. A rope was connected to each of these rollers and can be held down by a weight and pulled to move the chamber to east side of the chamber (see Figures 3 and S4).

Figure S2. The photograph shows the pulley system that lifts and collapses the bag in the ATMOX chamber.

S1.2 Chamber blackout blinds

Figure S3. The image shows the blackout curtains used in the ATMOX chamber. The loops sewn onto the blackout blinds wrap around the aluminum rods mounted at the top of the chamber.

S1.3 Light Characterization

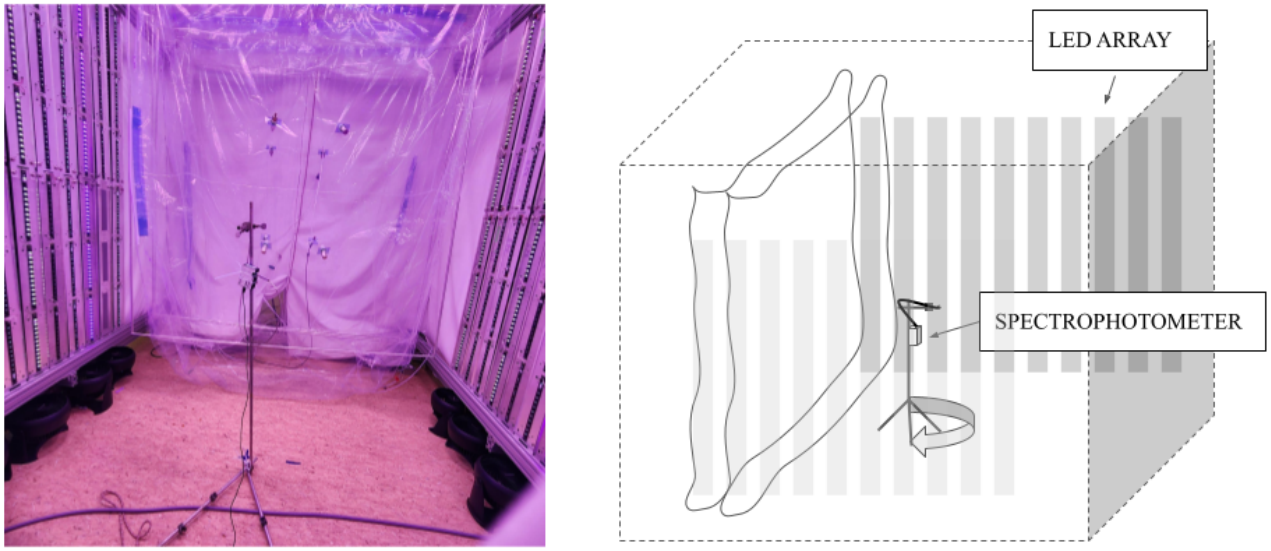

Figure S4. The experimental setup used to measure the absorbance spectra of the LEDs is pictures with all the LEDs on (left image) and as its corresponding schematic (right image). A tripod clamp was setup in the middle of the chamber with the spectrophotometer cosine receptor facing the side of measurement.

Figure S5. The photograph shows the LED bars (1 bar contains 12 LEDs) mounted on custom built aluminum panels. Then, three bars were wired in series on each panel, illustrating the electrical grouping used in ATMOX.

S1.4 Pillow bag

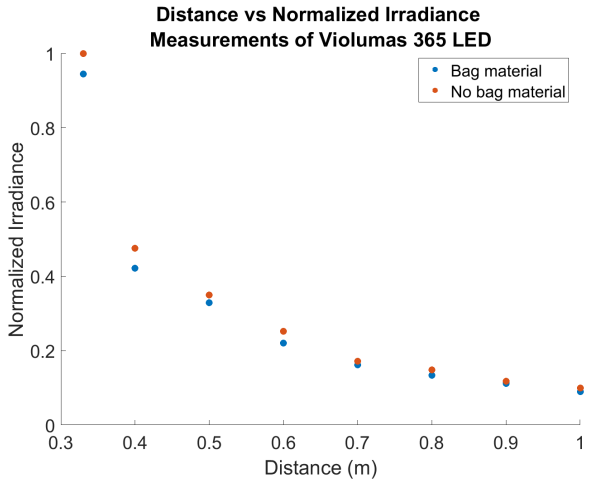

Figure S6. The spectrophotometer measurements of twelve 365 nm LEDs (1 bar) were made to quantify the transparency of the PFA material as a function of distance from the light. Based on these measurements, we determined that the bag material was transparent to approximately 94% to the LED output, thereby confirming that light transmission through the chamber is not a concern.

S1.5 Control Panel

To give the ATMOX chamber precise, wavelength-specific control, we built a compact panel in which each LED channel has three components: (i) a MAX472 display for real-time current read-out, (ii) a dedicated potentiometer for fine current tuning, and (iii) an on/off toggle switch. This setup lets the researcher select any combination of wavelengths, adjust their intensity to modulate reaction rates, and reliably reproduce the same lighting conditions from run to run.

The display modules have been modified to meet our needs. There is a power-ON/OFF toggle switch for the power supply. The potentiometer controls the output current, but because current drivers can behave unpredictably at exactly 0 A, a 10 kΩ series resistor ensures a small "idle" current even at the lowest setting. (The potentiometer is wired as a variable resistor and measures 91 kΩ at maximum.) The display modules are powered from a single 7.5–12 V supply (9 V recommended); each draws $\leq$ 0.1 A, so one supply can serve the entire panel. The wiring diagram for a single power supply and a single display module is in Figure S8. The same circuit was used for all power supplies in use. Additionally, the LEDs were wired in series of 3 sets as shown in Figure S5.

Current-display modules continuously monitor the currents of the LEDs as well as allow the adjustment of the output of each LED in tandem with a potentiometer. Ready-made MAX472 breakout boards were used with modifications depicted in Figure S8. Specifically, the modules needed modifications for two main reasons. First, we needed to add 4 diodes between the module return and the system ground since a +2.5 VDC bias above ground was required to operate properly in our setup. Secondly, we needed to isolate the low voltage power supply (9 V) from the LED panels' current path. The modification ensured that 9

V powered the module while being isolated from the LED current path. In Figure S8, the green lines show the original design from the purchased board, and the red lines represent our modifications. The modules work with 5-12 Vdc applied between DC+ and DC-Current sensing needs 3 or 4 diode drops (depending on the diode type) to lift the shunt circuit above ground. These diodes dissipate about 3.5 W of total power for currents of 1.4 A and half the power for currents of 0.7 A.

40 The MAX472 modules offer a quick on-board button routine for current-readout calibration; we used it to match the display to a reference current. The MAX472 board includes an optional relay output that can be user-programmed via its on-board buttons—to open or close when the measured current crosses one or two user-defined thresholds, effectively acting as a simple current-activated switch or alarm. This feature is intended for users who may want automatic over-current protection or visual indicators without additional electronics.

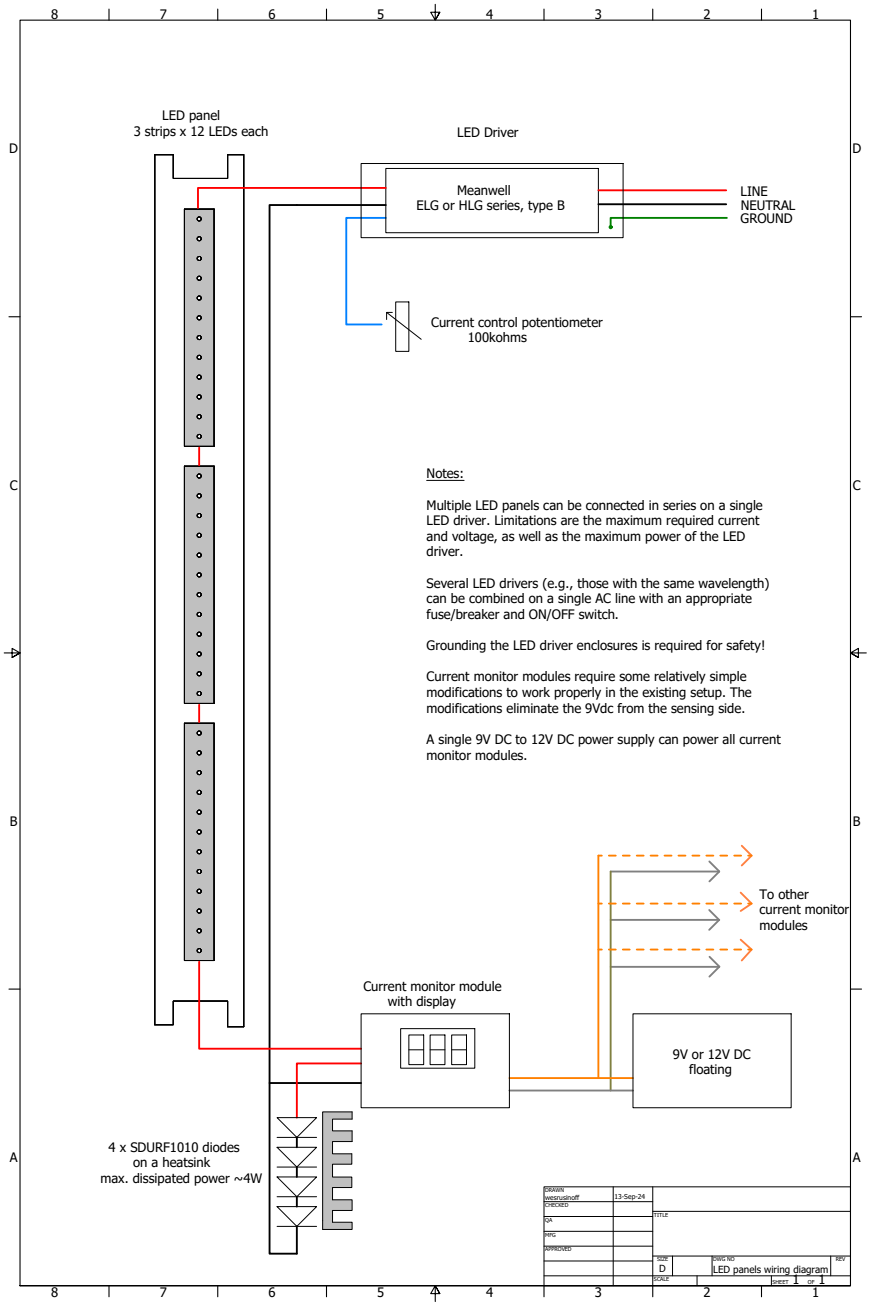

Figure S7. An LED driver (top box) sends steady power to a strip of LEDs. A knob (potentiometer) beside it lets the user turn the brightness up or down, while a small meter board shows the current on a digital display so the user always know how much power is flowing. The meter is protected by four safety diodes and is powered by an ordinary 9–12 V plug-in adapter that can also feed the other channels. More LED strips of the same colour can be added in line as long as the driver can handle the extra load, and every driver case was connected to ground for safety.

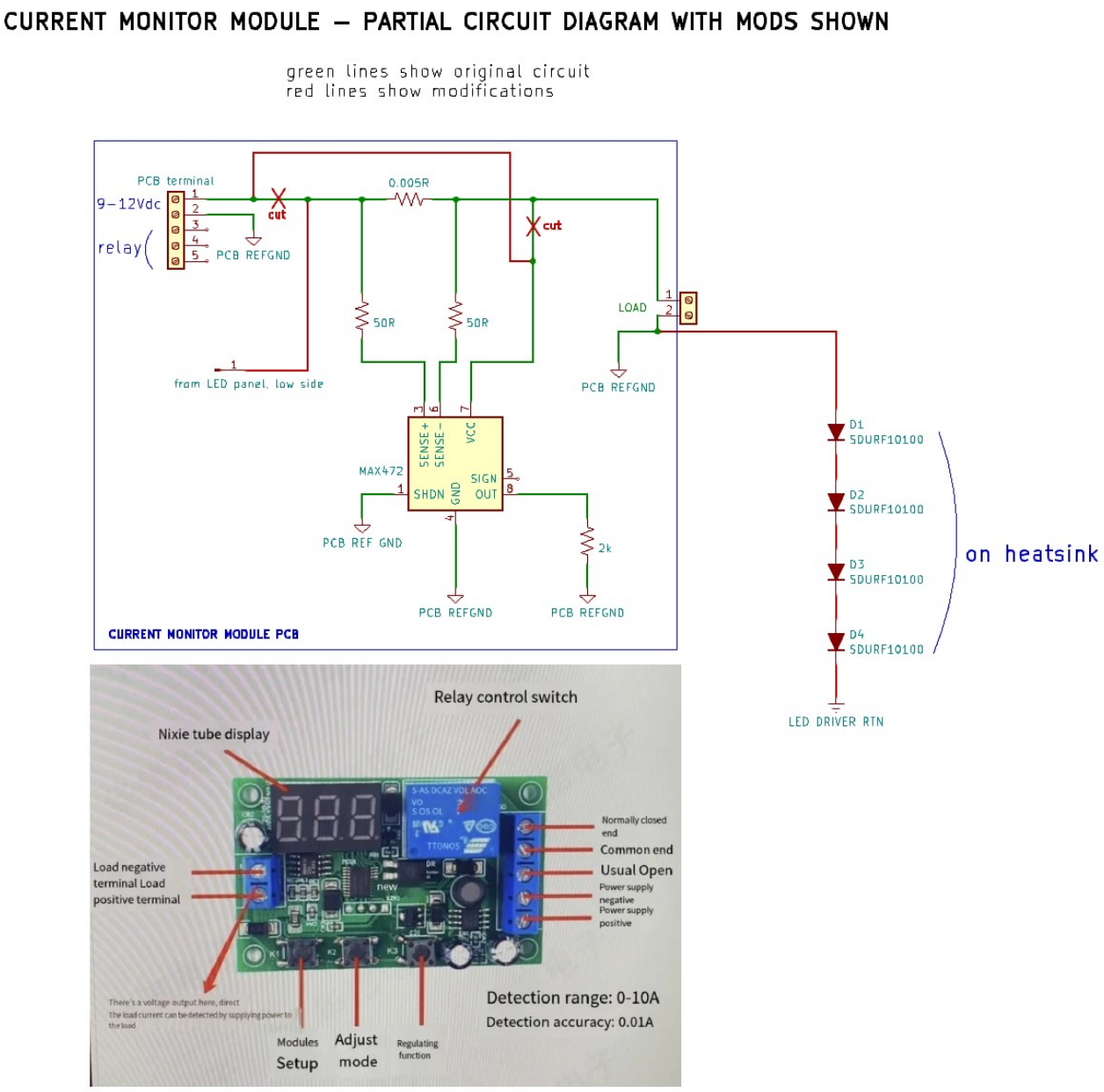

Figure S8. The top drawing shows the MAX472 module wiring schematic with our custom tweaks. Green lines trace the wiring that came on the bought-in board, while red lines show the two trace cuts marked by the X, and the jumper wire we added so the meter can read the LED current safely. Four diodes on the heatsink are placed to apply a +2.5 V bias so the current display module runs stable. The bottom photo shows the actual board after the changes. Labels point to the digital display, the three push buttons for setting the meter, the power terminals, and the relay header. The board also contains tiny display-control chips, a microcontroller, and voltage regulators that are left out here for clarity.

S1.6 LED orientation

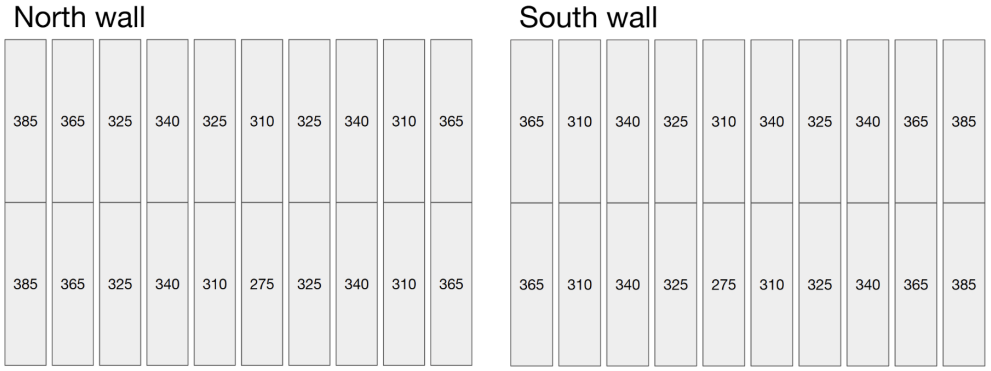

Figure S9. This diagram shows the placement of LED panels on the north and south walls, with each numbered box indicating the panel's peak wavelength in nm. Each rectangle has 3 LED bars which holds 12 LEDs per bar. This orientation was intended to space our the wavelengths and was used in the irradiance modeling in Figure 8a.

S2 LED Modeling

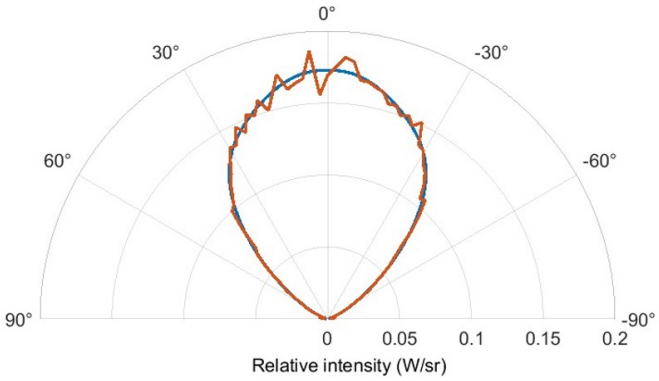

Figure S10. The red line traces the LED's measured radiation pattern, while the blue line shows the fitted cosine-power model. The pattern was approximated via the method used in Moreno and Viveros-Méndez (2021).

S3 Actinometry

To accurately characterize the LEDs in the ATMOX chamber, we monitored NO, NO_2, and O_3 under different irradiation conditions (Bohn et al. (2005)) (Figure 5 and Figure S11). The absorption cross-section of NO_2 spans the UV-B, UV-A, and visible

regions, matching our LED lights (275-385 nm). First, we inject NO_2 into the chamber, illuminate the chamber, measure the mixing ratios using gas analyzers, and subsequently calculate the rate, J_{NO_2}. The experiments last between 15 - 60 minutes depending on the light condition.

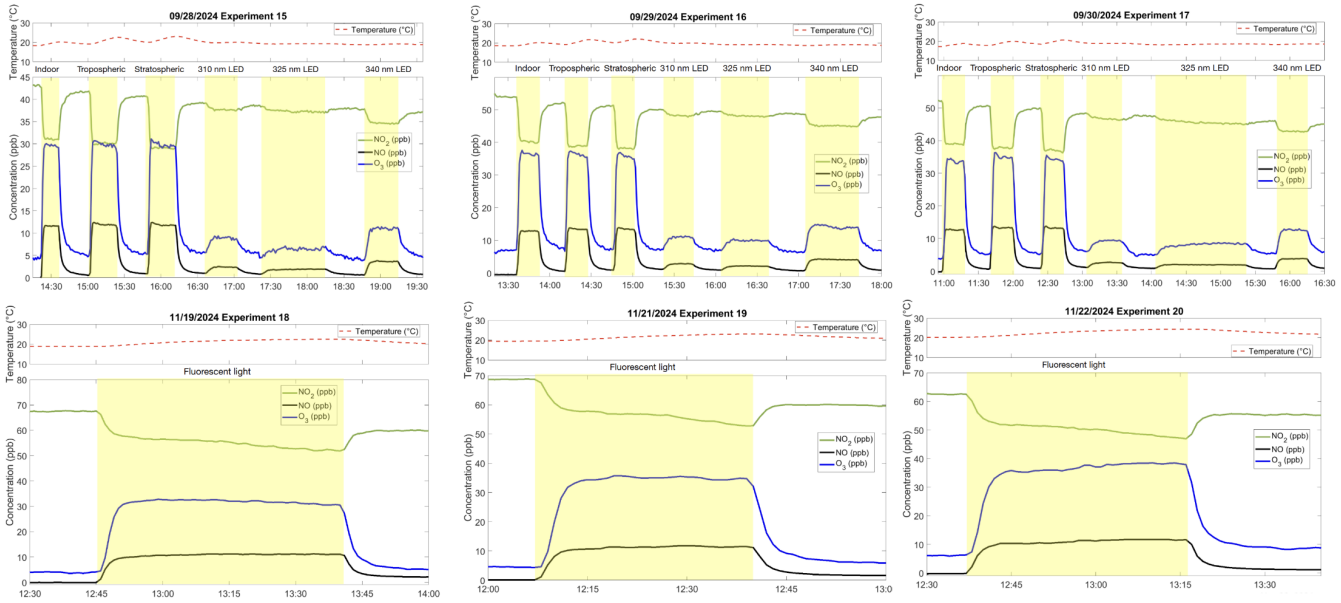

Figure S11. All actinometry experiment traces were performed in the ATMOX chamber while monitoring the trace gases and the temperature. Each subplot traces the temperature, and concentration of NO_2, NO, and O_3. The top panels correspond to experiments conducted under indoor, tropospheric, stratospheric, and single-wavelength lighting (310, 340, and 365 nm). The bottom figures represent fluorescent light experiments performed in a 0.45 m^3 PFA bag using fluorescent lights.

S3.1 Fluorescent experiments

Experiments in a PFA bag with fluorescent lights were performed to compare the relative performance of the LEDs.

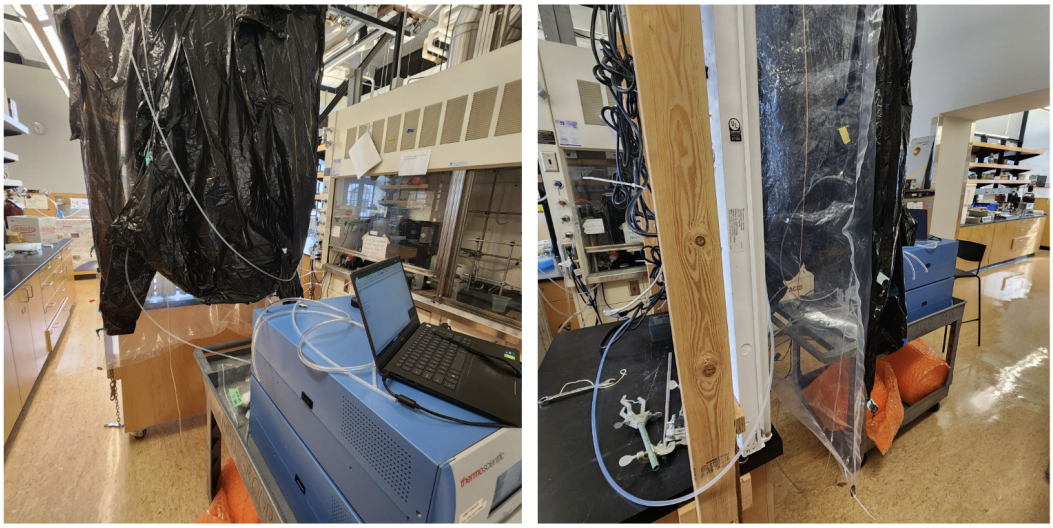

Figure S12. Actinometry measurements were performed on a 0.45 m^3 PFA bag using fluorescent lights. Photo on the left depicts the 42I and 49I gas analyzers, while the photo on the right depicts the side view of the fluorescent lights and pillow bag.

S3.2 J_{NO_2} intercomparison

Table S1. Comparison of J_{NO_2} values and their normalization per watt to other existing chambers that reported the details of their lights and J_{NO_2} values. Most chamber characterization report $_{NO_2}$ values, however only these few chambers also reported the light type where the consumption power could be determined based on the manufacturer specifications.

Chamber	Light Type	Light Model	J_{NO2} ($\times 10^{-3}$ s^{-1})	J_{NO2}/Watt ($\times 10^{-6}$)	Reference
ATMOX, UBC	LED	Violumas, FEIT	4.9	0.87	This study
AIR Chamber, PKU	Fluorescent	40 W, Bulb-T12, GE, USA	4.1	2.6	Zong et al. (2023)
BUCT	Fluorescent	60 W Philips 10R PL	6.0	1.9	Ma et al. (2022)
AIDA, KIT	LED	LEDs from LG Innotek, EPIGAP, Seoul Viosys, Osram	1.6	0.25	Vallon et al. (2022)
ILMARI, UEF	Fluorescent	36 W, Sylvania F36/T8 BLB	10.3	1.8	Leskinen et al. (2015)
PSI	Fluorescent	Cleo Performance solarium lamps, Phillips	8.0	2.0	Platt et al. (2013)

Table S2. List of J_{NO_2} photolysis rates under specified experimental conditions. Measurements under indoor, tropospheric, and stratospheric light were performed. Indoor conditions emit 365, 385, 450 nm light. Tropospheric conditions emit 310, 325, 340, 365, 385, and 450 nm light. Stratospheric conditions emit all the lights at 275, 310, 325, 340, 365, 385, 450 nm light. An additional measurement with fluorescent lights are also performed inside of a 450 L PFA bag.

Photolysis Experiment	O_3 (ppb)	NO (ppb)	NO_2 (ppb)	Temperature (°C)	J_{NO2} (s^{-1}, $\times 10^{-3}$)
Indoor light s1	29.8	11.6	30.8	20.2	4.44
Indoor light s2	35.9	13.0	40.2	20.2	4.59
Indoor light s3	33.3	12.5	33.9	18.2	4.72
Tropospheric s1	29.5	11.8	30.1	22.6	4.82
Tropospheric s2	35.6	13.3	39.0	21.7	4.95
Tropospheric s3	34.9	13.3	39.0	20.0	4.75
Stratospheric s1	29.5	11.7	29.1	23.1	4.93
Stratospheric s2	35.3	13.3	38.2	22.0	5.01
Stratospheric s3	34.2	13.2	37.0	20.6	4.86
Fluorescent s1	30.9	52.0	11.1	22.4	2.71
Fluorescent s2	34.9	52.9	11.5	23.1	3.14
Fluorescent s3	38.4	47.6	11.7	24.4	4.00

S4 Chamber cleaning

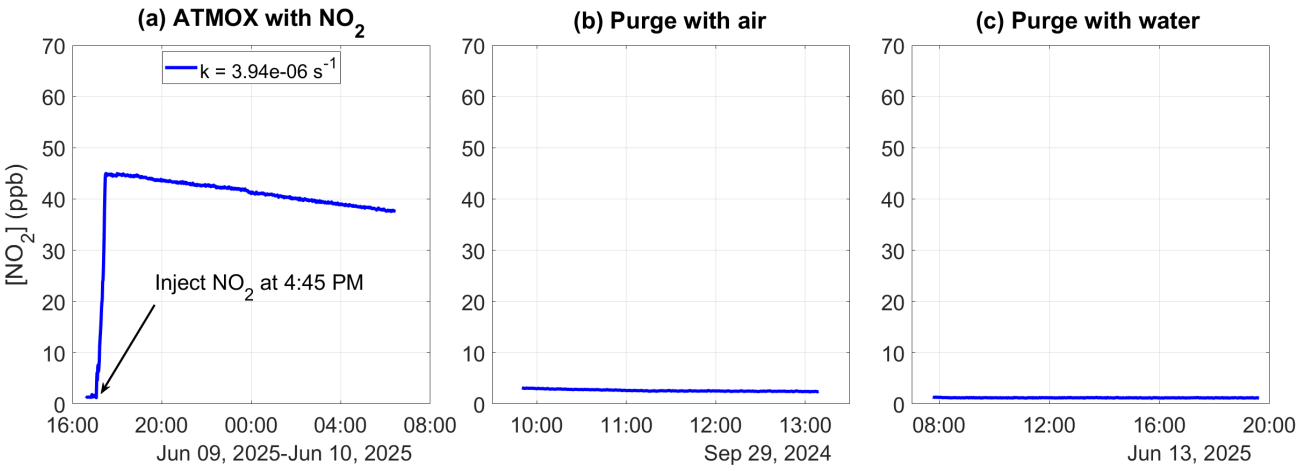

Figure S13. Time series of the evolution of NO_2 during an experiment (a), after purging overnight with clean air (b), and after cleaning with the pressure washer and water(c). The (a) panel also depicts the wall loss of NO_2 in an overnight experiment in our cubic 8 m^3. Purging with air (b) leaves a residual 2.6 ppb NO_2, whereas purging with water (c) cuts the background down to 1.2 ppb.

References

Bohn, B., Rohrer, F., Brauers, T., and Wahner, A.: Actinometric measurements of NO_2 photolysis frequencies in the atmosphere simulation chamber SAPHIR, Atmos. Chem. Phys., 5, 493–503, https://doi.org/10.5194/acp-5-493-2005, 2005.

Leskinen, A., Yli-Pirilä, P., Kuuspalo, K., Sippula, O., Jalava, P., Hirvonen, M.-R., Jokiniemi, J., Virtanen, A., Komppula, M., and Lehtinen, K. E. J.: Characterization and testing of a new environmental chamber, Atmos. Meas. Tech., 8, 2267–2278, https://doi.org/10.5194/amt-8-2267-2015, 2015.

Ma, W., Liu, Y., Zhang, Y., Feng, Z., Zhan, J., Hua, C., Ma, L., Guo, Y., Zhang, Y., Zhou, W., Yan, C., Chu, B., Chen, T., Ma, Q., Liu, C., Kulmala, M., Mu, Y., and He, H.: A New Type of Quartz Smog Chamber: Design and Characterization, Environ. Sci. & Technol., 56, 2181–2190, https://doi.org/10.1021/acs.est.1c06341, 2022.

Moreno, I. and Viveros-Méndez, P. X.: Modeling the irradiation pattern of LEDs at short distances, Opt. Express, 29, 6845–6853, https://doi.org/10.1364/OE.419428, 2021.

Platt, S. M., El Haddad, I., Zardini, A. A., Clairotte, M., Astorga, C., Wolf, R., Slowik, J. G., Temime-Roussel, B., Marchand, N., Ježek, I., Drinovec, L., Močnik, G., Möhler, O., Richter, R., Barmet, P., Bianchi, F., Baltensperger, U., and Prévôt, A. S. H.: Secondary organic aerosol formation from gasoline vehicle emissions in a new mobile environmental reaction chamber, Atmos. Chem. Phys., 13, 9141–9158, https://doi.org/10.5194/acp-13-9141-2013, 2013.

Vallon, M., Gao, L., Jiang, F., Krumm, B., Nadolny, J., Song, J., Leisner, T., and Saathoff, H.: LED-based solar simulator to study photochemistry over a wide temperature range in the large simulation chamber AIDA, Atmos. Meas. Tech., 15, 1795–1810, https://doi.org/10.5194/amt-15-1795-2022, 2022.

Zong, T., Wu, Z., Wang, J., Bi, K., Fang, W., Yang, Y., Yu, X., Bao, Z., Meng, X., Zhang, Y., Guo, S., Chen, Y., Liu, C., Zhang, Y., Li, S.-M., and Hu, M.: A new smog chamber system for atmospheric multiphase chemistry study: design and characterization, Atmospheric Measurement Techniques, 16, 3679–3692, https://doi.org/10.5194/amt-16-3679-2023, publisher: Copernicus GmbH, 2023.